Differentiation of derived rabbit trophoblast stem cells under fluid shear stress to mimic the trophoblastic barrier

Guenhaël Sanz, Nathalie Daniel, Catherine Archilla, Luc Jouneau, Yan Jaszczyszyn, Véronique Duranthon, Pascale Chavatte-Palmer, Alice Jouneau

▶ **To cite this version:**

Guenhaël Sanz, Nathalie Daniel, Catherine Archilla, Luc Jouneau, Yan Jaszczyszyn, et al.. Differentiation of derived rabbit trophoblast stem cells under fluid shear stress to mimic the trophoblastic barrier. Biochimica et Biophysica Acta (BBA) - General Subjects, 2019, 1863 (10), pp.1608-1618. 10.1016/j.bbagen.2019.07.003 . hal-02183790

HAL Id: hal-02183790
https://hal.science/hal-02183790v1

Submitted on 22 Feb 2023

HAL is a multi-disciplinary open access archive for the deposit and dissemination of scientific research documents, whether they are published or not. The documents may come from teaching and research institutions in France or abroad, or from public or private research centers.

L'archive ouverte pluridisciplinaire **HAL**, est destinée au dépôt et à la diffusion de documents scientifiques de niveau recherche, publiés ou non, émanant des établissements d'enseignement et de recherche français ou étrangers, des laboratoires publics ou privés.

BBA - General Subjects 1863 (2019) 1608–1618

Contents lists available at ScienceDirect

BBA - General Subjects

journal homepage: www.elsevier.com/locate/bbagen

Differentiation of derived rabbit trophoblast stem cells under fluid shear stress to mimic the trophoblastic barrier

Guenhaël Sanz[a,*], Nathalie Daniel[a], Marie-Christine Aubrière[a], Catherine Archilla[a], Luc Jouneau[a], Yan Jaszczyszyn[b], Véronique Duranthon[a], Pascale Chavatte-Palmer[a], Alice Jouneau[a,*]

[a] UMR BDR, INRA, ENVA, Université Paris-Saclay, 78350 Jouy-en-Josas, France
[b] Plateforme de Séquençage I2BC, CNRS, UMR9198, 91198 Gif-sur-Yvette, France

ARTICLE INFO

Keywords:
Trophoblast stem cell
Differentiation
Syncytiotrophoblast
Cell culture model
Fluid shear stress
Rabbit

ABSTRACT

Background: The placenta controls exchanges between the mother and the fetus and therefore fetal development and growth. The maternal environment can lead to disturbance of placental functions, with consequences on the health of the offspring. Since the rabbit placenta is very close to that of humans, rabbit models can provide biomedical data to study human placental function. Yet, to limit the use of animal experiments and to investigate the mechanistic aspects of placental function, we developed a new cell culture model in which rabbit trophoblast cells are differentiated from rabbit trophoblast stem cells.

Methods: Rabbit trophoblast stems cells were derived from blastocysts and differentiated onto a collagen gel and in the presence of a flow of culture medium to mimic maternal blood flow. Transcriptome analysis was performed on the stem and differentiated cells.

Results: Our culture model allows the differentiation of trophoblast stem cells. In particular, the fluid shear stress enhances microvilli formation on the differentiated cell surface, lipid droplets formation and fusion of cytotrophoblasts into syncytiotrophoblasts. In addition, the transcriptome analysis confirms the early trophoblast identity of the derived stem cells and reveals upregulation of signaling pathways involved in trophoblast differentiation.

Conclusion: Thereby, the culture model allows mimicking the *in vivo* conditions in which maternal blood flow exerts a shear stress on trophoblast cells that influences their phenotype.

General significance: Our culture model can be used to study the differentiation of trophoblast stem cells into cytotrophoblasts and syncytiotrophoblasts, as well as the trophoblast function in physiological and pathological conditions.

1. Introduction

The placenta controls exchanges between the mother and the fetus and therefore fetal development and growth. Furthermore, it is known that a deleterious maternal environment can lead to disturbance of placental functions, with consequences on the offspring health up to adulthood [1,2]. This is part of the concept of the "Developmental Origins of Health and Disease' (DOHaD). To decipher the molecular and cellular basis of perturbations of placental function, there is a need for *in vitro* models of trans-placental transfer. The part of the placenta mediating feto-maternal interactions originates from trophoblast cells, that are composed of cytotrophoblasts and syncytiotrophoblasts [3]. Up to now, most of the culture models developed to study the placental barrier use human primary cytotrophoblasts, which are laborious to purify and only grow for a few days, or choriocarcinoma cell lines, *i.e.*, cancerous cells further away from primary cells [4–13]. Among experimental animals, the rabbit has a placental structure closer to that of human placenta than other species regarding the chorion [14]. In the first half of gestation, a continuous internal layer of cytotrophoblasts and an outer layer of syncytiotrophoblast surround the chorionic villi of the human placenta [15]. At term, cytotrophoblasts remain present in patches but the syncytiotrophoblast remains intact. Thus, the human placenta is mostly considered as hemomonochorial although it is actually hemodichorial for more than half of the pregnancy [16]. The rabbit placenta is not villous as the human placenta but labyrinthine, and the trophoblast is composed of a syncytium and one layer of cytotrophoblasts. It is thus hemodichorial throughout pregnancy. The mouse placenta is also labyrinthine, but hemotrichorial since the

* Corresponding authors at: Biologie du Développement et Reproduction, INRA, ENVA, Université Paris-Saclay, 78350 Jouy-En-Josas, France.
E-mail addresses: guenhael.sanz@inra.fr (G. Sanz), alice.jouneau@inra.fr (A. Jouneau).

https://doi.org/10.1016/j.bbagen.2019.07.003
Received 15 April 2019; Received in revised form 18 June 2019; Accepted 2 July 2019
Available online 03 July 2019
0304-4165/ © 2019 Elsevier B.V. All rights reserved.

trophoblast is composed of a layer of cytotrophoblasts in contact with maternal blood, covering two layers of syncytiotrophoblast [17,18], which makes it structurally less pertinent than the rabbit as a model for human placenta. Here, we developed a new cell culture model in which rabbit trophoblast stem cells are differentiated into cytotrophoblasts and syncytiotrophoblasts in order to work with cells close to primary cells. A flow of medium exerting a shear stress over the culture was shown to promote trophoblast cell differentiation and function, favoring the formation of microvilli on the cell surface in BeWo human choriocarcinoma cells [6,11] and production of placental growth factor in primary human placental cells [19]. Microvilli formation induced by fluid shear stress (FSS) was reported to result from a mechanosensitive activation of the vanilloid family type-6 (TRPV6) channels, leading to Ca^{2+} influx and consecutively to Akt and Ezrin phosphorylation [11,20,21]. Regarding the production of placental growth factor induced by FSS, it results from an increase in Ca^{2+}, leading to enhancement of PGE2 production that could stimulate a cAMP-PKA signaling pathway [19]. Based on these data, we decided to derive trophoblast stem cells from rabbit blastocysts and to differentiate them using a culture system with FSS. We characterized cells developed using this system and analyzed their transcriptome along the differentiation process. Such an *in vitro* model system will be highly relevant to investigate the mechanisms of trophoblast differentiation and its perturbations, as well as the functional defects of differentiated trophoblasts induced by certain environmental disturbances.

2. Materials and methods

2.1. Ethical statement

All experiments were performed in accordance with the International Guiding Principles for Biomedical Research involving animals as promulgated by the Society for the Study of Reproduction and in accordance with the European Convention on Animal Experimentation. The animal experimental design was carried out under the approval of national ethic committee (APAFIS #2180-2015112615371038v2) and under the approval of the local ethic committee (Comethea n°45, registered under n° 12/107 and n°15/59).

2.2. BeWo cell culture

BeWo cells (passage 9) were kindly provided by Dr. T. Fournier (Faculté de pharmacie de Paris, France) and grown in RPMI1640 containing glutamax (Gibco) supplemented with 10% fetal bovine serum (FBS) (Gibco) at 37 °C in a humidified incubator with 5% CO_2. BeWo cells were seeded at a density of $1{,}9.10^5$ cells / cm^2 onto a collagen type I (Corning) gel prepared as described previously [22]. The collagen matrix was jellified on the bottom of 35 mm diameter culture dishes (75 µL / cm^2). Once the cells had adhered to the collagen gel, a flow of culture medium of 0.5 mL/min was applied for 96 h in closed circuit into the dish using a peristaltic pump (Ismatec REGLO). This flow rate resulted in a shear stress in the range of physiological values estimated for the human placenta, between 0.001 and 1 $dyn.cm^{-2}$ according to blood flow heterogeneity in the placenta and to various authors [11,23,24] (see estimation of FSS values in supplementary Material). For cells grown in static conditions (without medium flow), two-thirds of the culture medium were renewed every day so that cells did not lack nutrients while remaining in contact with the factors they secreted.

2.3. Preparation of mouse embryonic fibroblasts (MEFs) conditioned medium

Mitomycine C-inactivated MEFs were seeded at a density of $3.2.10^4$ cells / cm^2, in 0.18 mL / cm^2 of basic medium (RPMI1640 containing glutamax (Gibco),1 mM sodium pyruvate (Gibco), 20% FBS (Hyclone)). The culture medium was then collected and renewed every three days during nine days. The collected conditioned medium was centrifuged to remove floating cells and stored at −80 °C in aliquots of equivalent volume. When the conditioned medium was used, an aliquot of each of the three collections was thawed and the three aliquots were pooled.

2.4. Derivation of rabbit trophoblast stem cells (rTSCs)

Rabbit trophoblast stem cells were derived from blastocysts obtained from New Zealand White female rabbits (20–22 weeks old) which were super-ovulated prior to mating. Blastocysts were collected from uteri perfused with PBS (Gibco) at 96 h post-coïtum (hpc). The mucin coat and the zona pellucida of the rabbit blastocysts were mechanically removed after brief exposure (2 min) to 5 mg/mL pronase (Sigma). Four to five blastocysts were pooled in one well of a 4-well cell culture plate (Nunc) and incubated at 38,5 °C in a humidified incubator with 5% CO_2 and in 500 µL of the following rTSCM medium: 30% of basic medium, 70% of conditioned medium, 100 µM β-mercaptoethanol (Gibco), 25 ng/mL FGF1 (Merck), 25 ng/mL FGF2 (Merck), 5 ng/mL TGFβ1 (Merck) and 1,5 µg/mL heparin (Sigma). The outgrowths were dissociated after five days using TrypLE Select (Gibco) and replated under the same conditions. Then, cells were passaged every two days using TryPLE Select. rTSCs were considered to be stably established when morphology was homogenous, after 10 passages.

2.5. Differentiation of rTSCs

rTSCs were seeded in basic medium at a density of $1.6.10^4$ cells / cm^2 onto a collagen type I (Corning) gel prepared as described previously [22]. The collagen matrix was gelified in 12-well plates or on the porous membrane of transwells (NuncTM polycarbonate cell culture inserts, 0.4 µm pore size) in 6-well plates (400 µL per well or transwell). Cells were grown in the basic culture medium at 38,5 °C in a humidified incubator with 5% CO_2. After 4 days of culture, a flow of culture medium was applied in closed circuit into the well (or into the upper compartment of the transwell) using a peristaltic pump (Ismatec REGLO) and for 48 h. To determine the flow rate to apply on rTSCs, various flow rates were tested (0.1, 0.2 and 0.5 mL/min). For cells grown in static conditions (without medium flow), two-thirds of the culture medium were renewed every day so that cells did not lack nutrients while remaining in contact with the factors they secreted. In order to assess the impact of growing cells onto a collagen matrix and with a flow of culture medium, rTSCs were also grown in conditions lacking a collagen gel and without a flow of culture medium. For that, they were first grown for 3 days until confluence and then seeded at a 1/10 dilution and grown for 4 additional days.

2.6. Calcium imaging

rTSCs were grown in a 96-well culture plate (black microtiter plate, Greiner Bio-one) at a density $1.6.10^4$ cells / cm^2 and onto a collagen I gel (40 µL / well). After 4 days of culture in the basic medium, intracellular calcium was measured with or without FSS. For that, cells were loaded with 2.5 µM of Fluo-4 acetoxymethyl ester (Molecular Probes) as described in [25]. Calcium imaging was performed using an inverted epifluorescence microscope (CK40 Olympus) equipped with a digital camera (ORCA-ER, Hamamatsu Photonics). Ca^{2+} responses were observed at 460–490 nm excitation and ≥ 515 nm emission wavelengths. Data acquisition was performed using the HCimage software (Hamamatsu) during three minutes, without medium flow, or with a flow rate of 0.15 mL/min corresponding to an estimated FSS value between the estimated FSS values for flow rates of 0.2 or 0.5 mL/min in a 12-well plate. The medium flow was applied with an engineered perfused top as in [26]. The Ca^{2+} signal was measured as the relative change in fluorescence intensity $\Delta F/F = (Fmax-F0)/F0$, where Fmax is the maximum fluorescence intensity and F0 is the fluorescence intensity before the intracellular calcium rise. Three independent experiments

were performed with four replicates for each conditions. ΔF/F was calculated in 200 cells for each condition (with or without flow).

2.7. Cell component staining

Before staining various cell components, cells were fixed with 4% paraformaldehyde in PBS (for 20 min at 20 °C), permeabilized with 0.5% Triton X-100 in PBS (for 15 min at 20 °C), and a saturation was performed using 2% BSA in PBS (for 30 min at 20 °C). Cells were washed three times with PBS after each step.

To delineate cell shape, actin was stained using 4 U/mL Rhodamine Phalloïdin (Invitrogen) in PBS. Cells were incubated for 30 min at 37 °C with Rhodamine Phalloïdin, then washed five times with PBS.

To observe lipid droplets, they were stained using 3 μg/mL Bodipy 493/503 (Molecular Probes) in PBS. Cells were incubated for 15 min at 20 °C with Bodipy 493/503, then washed five times with PBS.

To detect cell nuclei, 2 μg/mL DAPI (Invitrogen) was added to the Citifluor (Biovalley) antifading solution used for confocal microscopy observations.

Once the various cell markings were performed, the collagen gel carrying the cells was placed between a slide and a coverslip in Citifluor and cells were observed by confocal microscopy under a Zeiss LSM 700 confocal microscope at a 40× magnification (MIMA2 platform, INRA).

3. hCG-β immunodetection in BeWo cells

Cells were first fixed with 4% paraformaldehyde in PBS (for 20 min at 20 °C) and permeabilized with 0.5% Triton X-100 in PBS (for 15 min at 20 °C). Saturation was then performed using 2% BSA in PBS (for 1 h at 20 °C). hCG-β production in BeWo cells was assessed using a primary hCG-β antibody (Clinisciences AP13036b) diluted 1/250 in PBS containing 2% BSA (overnight at 4 °C) and a secondary fluorescent antibody (FITC anti-rabbit antibody, Jackson ImmunoResearch) diluted 1/200 in PBS containing 2% BSA (for 1 h at 20 °C).

3.1. Assessment of microvilli formation

To quantify microvilli formation on the cell surface, the area occupied by the microvilli was measured in orthogonal sectional views ($n = 20$) of various microscopic fields using the Image J software. These measurements were semi-quantitative due to approximations of the microvilli area.

3.2. Lipid droplets quantification

To quantify lipid droplet formation, their number and size were measured in various microscopic fields ($n = 15$) of two independent experiments using the imageJ software.

3.3. Assessment of cell fusion

Syncytiotrophoblasts resulting from the fusion of cytotrophoblasts were observed by confocal microscopy (Zeiss LSM-T-PMT confocal microscope, 40× magnification) and identified as multinucleated cells according to the actin and nuclei staining. For BeWo cells, since cell fusion was not very extensive (essentially between two cells), it was assessed by counting the multi-nucleated cells in various microscopic fields ($n = 7$, results were normalized taking into account total cell number in each field) of two independent experiments. For rabbit trophoblast cells, since cell fusion was more extensive, possibly resulting from the fusion of more than two cells, it was assessed by measuring the mean surface of syncytiotrophoblasts in various microscopic fields ($n = 15$) of two independent experiments. Measurements were performed using the ImageJ software.

3.4. Assessment of cell layer permeability

Rabbit trophoblast cells were differentiated on a collagen matrix onto the porous membrane of a transwell as described above, with or without FSS (flow rate of 0.2 mL/min). To measure cell layer permeability, 0.1 mg/mL FITC-Dextran (PM 3000, Invitrogen) was added in the upper compartment of the transwell and measured in the culture media at different times using a multimode microplate reader (TriStar, Berthold Technologies). Results are shown as the amount (%) of FITC-Dextran transferred from the upper to the lower compartment of the transwell over time for 3 h. Two biological replicates each with two technical replicates were performed.

3.5. RNA isolation

Total RNAs from rabbit trophoblast cells were prepared using the RNeasy Kit (Qiagen). For cells grown onto a collagen gel, extraction of the cells from the collagen gel was performed before performing RNA isolation, as described previously [27]. Briefly, cells were washed twice with cold PBS and the collagen gel in cold PBS was transferred into a 1.5 mL tube. The collagen gel was fragmented by gently pipetting and the suspension was centrifuged at 7500 rpm for 1 min at 4 °C. The PBS and the collagen phase were removed to keep the cell pellet.

To isolate RNAs from the trophectoderm of blastocysts (96 hpc), the trophectoderm was separated from the inner cell mass (ICM) by immunosurgery. For this purpose, after chemical and mechanical removing of the mucin coat and zona pellucida, blastocysts were first incubated in TCM199 supplemented with 10% FBS until they recovered a normal morphological aspect, then in an anti-rabbit whole goat serum (Sigma R-5131) at 37 °C for 60 to 90 min and exposed (5 min) to guinea pig complement serum (Sigma S-1639). The ICM was then mechanically dissociated from the trophectoderm. Samples were pooled by 10 and dry frozen. Total RNAs from batches of trophectoderms (20 trophectoderms from 96 hpc blastocysts, 3 replicates) were extracted using the PicoPure RNA extraction kit (Arcturus).

In all cases, DNAse I (Qiagen) treatment at 25 °C for 15 min was performed prior to RNA elution. RNAs were checked for quality and quantified using an Agilent 2100 Bioanalyzer and a RNA 6000 pico kit (Agilent Technologies). RNA Integrity Numbers (RIN) were between 9.5 and 10.

3.6. RNA sequencing

Three nanograms of total RNA were used for amplification using the SMART-Seq V4 ultra low input RNA kit (Clonetech) according to the manufacturer's recommendations (10 PCR cycles were performed). cDNA quality was assessed on an Agilent Bioanalyzer 2100, using an Agilent High Sensitivity DNA Kit. Libraries were prepared from 0.15 ng cDNA using the Nextera XT Illumina library preparation kit. Libraries were pooled in equimolar proportions and sequenced (Paired-end 50–34 pb) on an Illumina NextSeq500 instrument, using a NextSeq 500 High Output 75 cycles kit. Demultiplexing was performed (bcl2fastq2 V2.2.18.12) and adapters were trimmed with Cutadapt1.15, so that only reads longer than 10 bp were kept.

3.7. Transcriptomic analyses

Reads were mapped to the rabbit genome (*Oryctolagus cuniculus* 2.0) using the splice junction mapper TopHat (version 2.0.14) associated with the short-read aligner Bowtie2 (version 2.1.0). Finally, featureCounts (version 1.4.5) was used to establish gene count table. Hierarchical clustering was computed using hclust R package, Euclidean distance metric and Ward linkage. Principal Component analysis was made using FactoMineR [28]. Data normalization and single-gene level analysis of the differential expression were performed using the DESeq2 [29]. Differences were considered significant for

adjusted P values (Benjamini-Hochberg) ≤ 0.05, and absolute fold change ≥ 2. Log2 transformed read counts (Rlog) (after normalization by library size) were obtained with DEseq2 package and used for heatmaps and expression dot plots.

Gene Ontology (GO) terms and Kyoto Encyclopedia of Genes and Genomes (KEGG) pathways enrichment analysis was performed using DAVID [30].

RNA-seq data are deposited in NCBI SRA with the accession number PRJNA529333.

3.8. Statistical analyses

To compare different cell culture conditions, a Kruskal-Wallis test was first performed and then all pairs of groups were compared using a Mann Whitney test. Results were considered significant for P values ≤ 0.05.

4. Results and discussion

4.1. Derivation of rabbit trophoblast stem cells (rTSCs)

In the present study, rTSCs were derived from rabbit blastocysts that were collected 96 h post-coïtum. Blastocysts were explanted *in vitro* and cultured in the presence of serum, MEF conditioned medium and TGFβ1 as for mouse TSCs [31,32], as well as several FGF family members (FGF4 alone or a combination of FGF1 and FGF2). We found that the combination of FGF1, FGF2 and TGFβ1 enabled derivation and maintenance of rTSCs as previously reported [33]. In addition, we only succeeded in deriving rTSCs when pooling several blastocysts in a single well. In these conditions, the blastocyst inner cell masses degenerated within a few days while the trophectoderm-derived cells proliferated (Fig. 1A, B). Once established, rTSCs were maintained up to twenty passages without apparent morphological changes (Fig. 1C). Two independent lines (rTS_A and rTS_B) were derived and used throughout this study. Furthermore, a third line (rTS_C) was sub-cultured from rTS_B culture and then expanded independently.

4.2. Differentiation of rTSCs under fluid shear stress

We first used BeWo cells to check that our culture conditions enabled us to reproduce previously published results, especially that growing cells under a fluid shear stress promotes the formation of microvilli on the cell surface. As expected and shown in supplementary Figs. 1A and 2A, we observed more microvilli on the surface of BeWo cells grown under FSS. We also noticed that the medium flow promoted the fusion between cells and production of hCG-β by the fused cells (supplementary Fig. 1B, C and D). The production of hCG-β during human trophoblast differentiation and by the syncytiotrophoblast has already been described [34] and was shown to be under the control of the nuclear receptor PPARγ [35,36]. Hence, cell fusion together with hCG-β production indicates that our cell culture system using FSS is able to promote trophoblast cell differentiation into syncytiotrophoblast like cells. Moreover, according to our knowledge, albeit the cell fusion and hCG-β production that we observed in BeWo cells were not very extensive, this is the first time that they are reported as induced by fluid mechanical forces.

We then used this culture system to differentiate rTSCs. Cells were cultured on collagen without growth factors nor conditioned medium. FSS was applied when the cell layer was nearly confluent. We again observed more microvilli on the cell surface in the presence of flow (Fig. 2A and supplementary Fig. 2B). Furthermore, as for BeWo cells, we observed increased cell fusion under FSS (Fig. 2B and C) and this was more pronounced for the flow rates 0.2 mL/min and 0.5 mL/min. Yet, in the case of rabbit trophoblast cells, the fusion occurred between more than two cells, while in the case of BeWo cells it was mainly a fusion of only two cells (compare Fig. 2B and supplementary Fig. 1D). We thus stipulate that trophoblast cells differentiated from tissue stem cells achieve a more differentiated state, notably under FSS, than cancer-derived cells. To further assess the formation of a syncytium and the disappearance of intercellular spaces, we used FITC-Dextran transfer as a measure of cell layer permeability. We demonstrated that the increased cell fusion to form syncytiotrophoblasts was accompanied by a reduction of FITC-Dextran transfer and thus of cell layer permeability (Fig. 2D). Moreover, the flow increased the accumulation and size of lipid droplets inside the cells, with a stronger effect for the flow rates 0.2 mL/min and 0.5 mL/min (Fig. 2B and E). Such accumulation of lipid droplets during differentiation of cytotrophoblasts and fusion of cytotrophoblasts to form syncytiotrophoblasts have already been reported in human trophoblast cells and controlled by the nuclear receptor PPARγ [36,37].

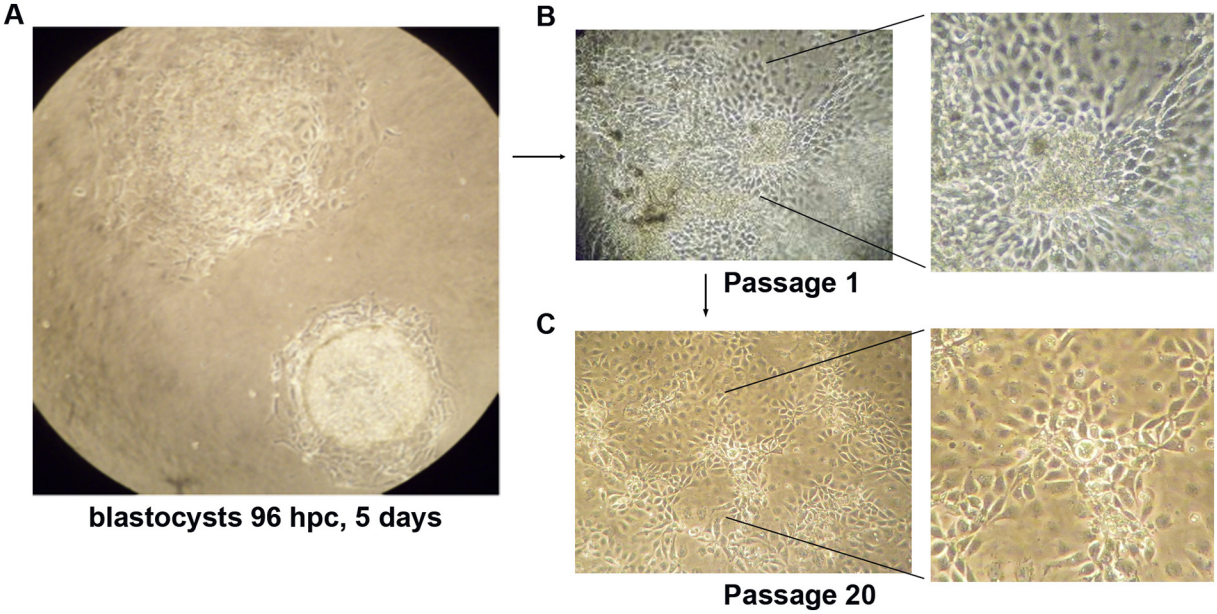

Fig. 1. Derivation of rabbit trophoblast stem cells. A) Blastocysts collected 96 h post-coïtum and grown in rTSCM for 5 days. B) Heterogenous cell population at passage 1. C) rTSCs at passage 20 showing a homogeneous morphology.

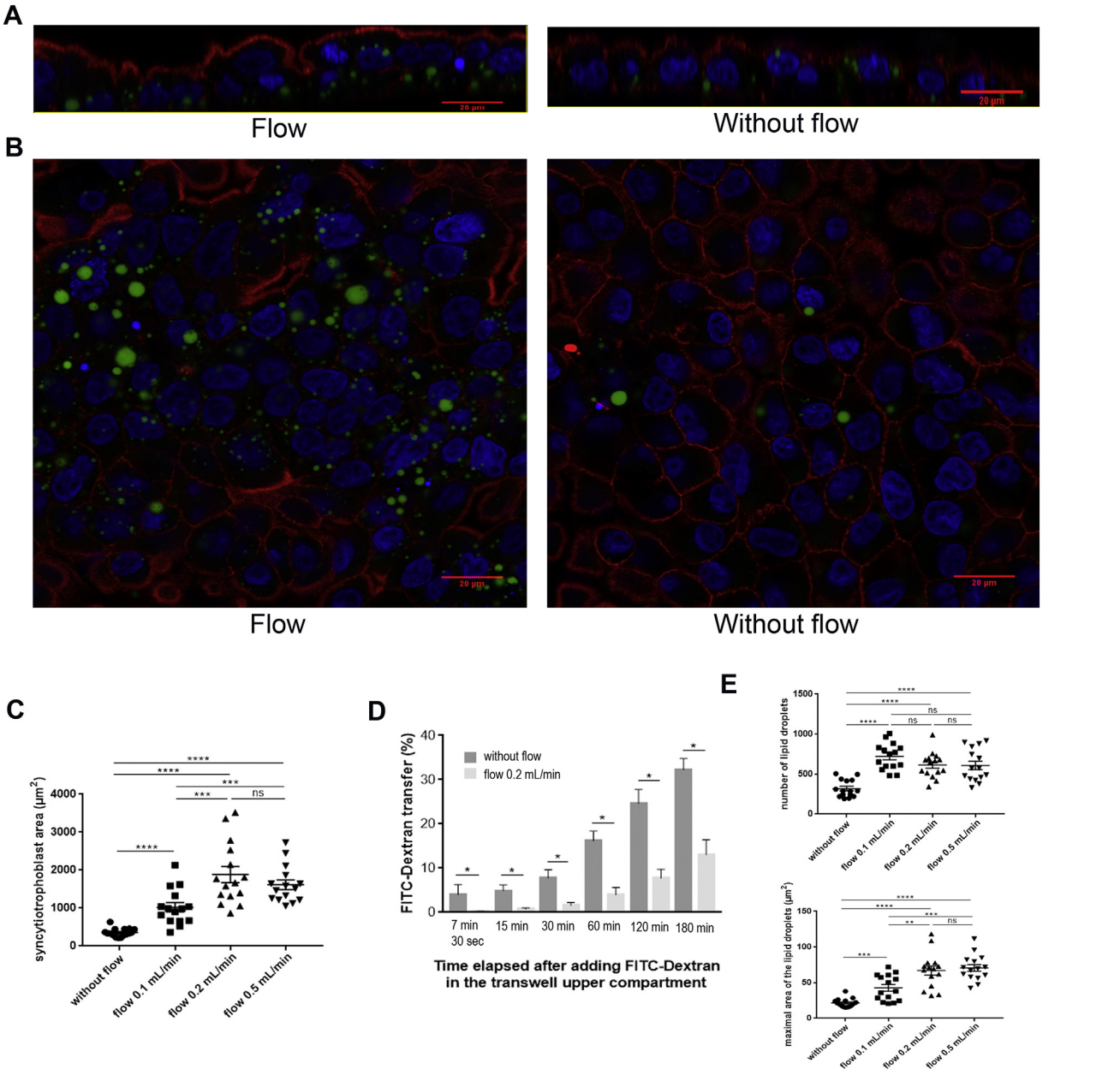

Fig. 2. Fluid shear stress effects on rabbit trophoblast cells: enhancement of microvilli formation on the cell surface, cell fusion and accumulation of lipid droplets. A) Orthogonal sectional views after *Z*-stack acquisition by confocal microscopy of rabbit trophoblast cells grown onto a collagen I gel with or without fluid shear stress (FSS). Actin appears in red (Rhodamine phalloïdin), nuclei in blue (DAPI) and lipid droplets in green (Bodipy 493/503). Microvilli appear as small bristles on the cell surface (in red). B) 2D images of rabbit trophoblast cells grown onto a collagen I gel with or without FSS and observed by confocal microscopy. Actin appears in red (Rhodamine phalloïdin), nuclei in blue (DAPI) and lipid droplets in green (Bodipy 493/503). Fused cells are multi-nucleated cells (several nuclei surrounded by a single continuous actin marking). C) Assessment of rabbit trophoblast cell fusion per microscopic field as syncytiotrophoblast (multi-nucleated cells) area. D) Assessment of cell layer permeability to FITC-Dextran. Results are shown as the cumulative amount (%) of FITC-Dextran transferred from the upper to the lower compartment of a transwell at different time points. Cells were grown onto a collagen I gel which covered the porous membrane of the transwell, with or without FSS. E) Quantification of lipid droplet accumulation inside the cells per microscopic field. Lipid droplets were detected using Bodipy 493/503 (see panel B) and their number and size determined.

Given these results, flow rates ranging from 0.2 to 0.5 mL/min were able to enhance the differentiation of rabbit cytotrophoblasts while a flow rate of 0.1 mL/min was less efficient. To our knowledge, there is no available data on FSS in the rabbit placenta. Yet, the flow rate of 0.5 mL/min corresponds to a physiological shear stress in the human placenta [23] and 0.2 mL/min is near the lowest reported value. Hence, we speculate that FSS exerted by flow rates between 0.2 and 0.5 mL/min correspond to a physiological shear stress in the rabbit placenta, similar to that in the human placenta.

So far, in the case of BeWo cells, cell fusion was only observed after treatment with forskolin or cAMP [6,9,38]. Since FSS induces cAMP production by trophoblast cells through Ca^{2+} increase and consecutive stimulation of PGE2 production [19,39], its ability to promote trophoblast cell fusion could be expected. Moreover, in the placenta, PGE2 was reported to be transformed into 15-keto-PGE2 [40], which is itself a ligand of PPARγ [41]. PPARγ is a known regulator of trophoblast cell differentiation, and in particular of syncytiotrophoblast formation and lipid accumulation [37,42]. In addition, cAMP stimulates PPARγ activity [35] and PPARγ upregulates the transcriptional activity of GCMa, and consequently the expression of syncytin-1, which mediates

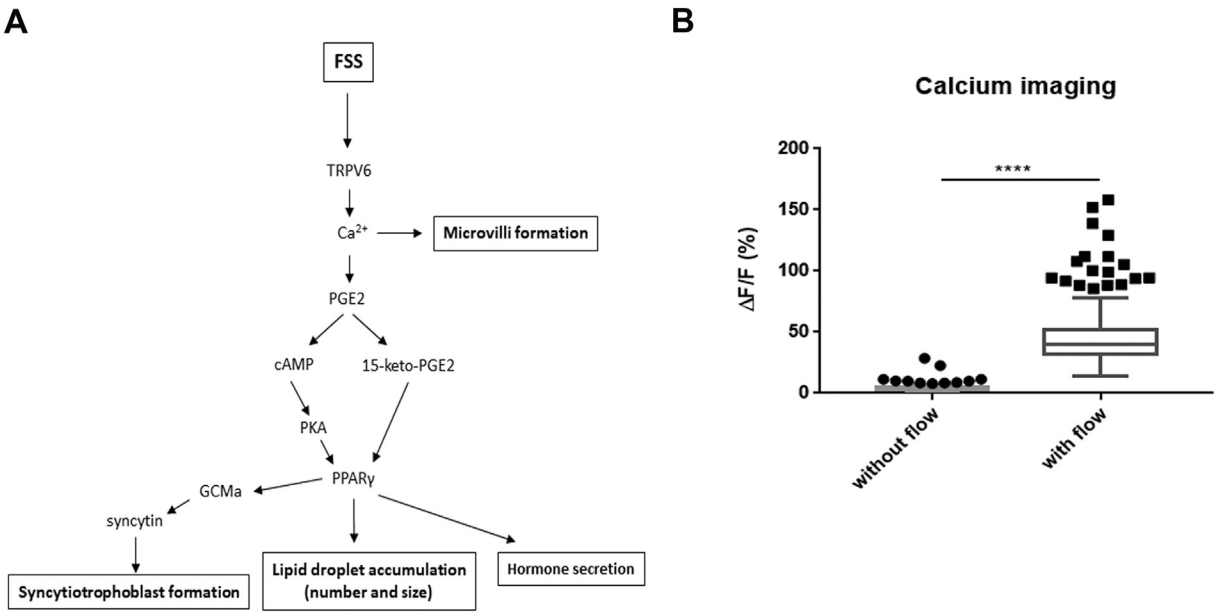

Fig. 3. A) Proposed cell signaling network to explain fluid shear stress effects on trophoblast cells. Fluid shear stress (FSS) was described to activate TRPV6 channels, resulting in increased intracellular Ca^{2+} levels, which promotes various cellular effects such as microvilli formation on the cell surface and PGE2 production. PGE2 was reported to activate adenylate cyclase and thereby to increase intracellular cAMP levels, leading to increased PPARγ activity. PGE2 was also described as being transformed into 15-keto-PGE2 in the placenta, the latter being a PPARγ ligand. Thus, FSS seems to regulate PPARγ activity, which in turn promotes hormone secretion, lipid droplet accumulation and syncytiotrophoblast formation. In the latter case, PPARγ enhances GCMa transcriptional activity, leading to an increase in the expression of syncytin, which mediates the fusion of cytotrophoblasts into syncytiotrophoblasts. B) Calcium imaging performed on trophoblast cells differentiated onto a collagen I gel. Cells were loaded with Fluo-4 acetoxymethyl ester, and Ca^{2+} responses were observed during three minutes, without flow or with a flow rate of 0.15 mL/min. The Ca^{2+} signal was measured as the relative change in fluorescence intensity (ΔF/F) for 200 cells in both conditions. Results are shown as a Tukey box plot.

cell fusion [43–46]. Taken together, these data led us to propose a signaling network (Fig. 3A) originating from FSS stimulation and regulating the various trophoblast features, such as microvilli formation, cell fusion to form syncytiotrophoblasts, hormone production and lipid accumulation, that we have observed in our study. We also performed calcium imaging experiments using differentiated trophoblast cells on collagen matrix to show that the mechanical forces exerted by a flow of culture medium were able to induce an increase in intracellular calcium that could lead to the signaling pathways suggested in Fig. 3A. The results of Fig. 3B show that the FSS indeed induced an increase in intracellular calcium, with a mean fluorescence variation close to 50% in the differentiated trophoblast cells under FSS, as reported by other authors [11,19].

In the placenta, maternal blood flow exerting mechanical forces on trophoblast cells could induce such signaling network triggered by mechanotransduction. The syncytiotrophoblast layer is a major site of materno-fetal exchanges in the hemochorial placenta (such as rabbit or human placenta) and also possesses an essential endocrine function to sustain gestation [47]. Microvilli formation is essential to increase the exchange surface of trophoblast cells in contact with maternal blood, favoring transplacental transfers to the fetus. Lipid droplet accumulation in trophoblasts allows the placenta to transfer lipids to the fetus [48], with a major role in fetal growth [49]. In preeclamptic women, the disturbance of blood flow may be expected to affect the differentiation and function of the placenta through changes in the mechanical forces exerted on trophoblast cells [23], which could lead to fetal growth restriction. In this context, our culture model could provide a useful tool to investigate some features and impacts of preeclampsia, in particular regarding the structure and function of the placental syncytium, known to be altered in preeclampsia [50], although preeclampsia does not occur spontaneously in rabbits.

4.3. Transcriptome analyses of rTSCs and their differentiated progenies

To get further insights into the identity of the rTSCs and the changes during their differentiation into syncytiotrophoblasts, we analyzed the transcriptomes of rTSCs, their tissue of origin (trophectoderm at 96 hpc) and of the trophoblast cells differentiated in various conditions (simple differentiation procedure without collagen nor flow, and on collagen I gel with and without FSS).

Clustering of all samples revealed that rTSCs were well separated from the tissue of origin, the trophectoderm, but also from the differentiated progeny (Fig. 4A). The tight grouping of the different rTSCs samples indicates that they had a stable transcriptome in the three expanded cell lines (in Fig. 4, rTS_A are independent from rTS_B and rTS_C. rTS_B and rTS_C are from the same derivation but expanded independently) and along passages (in Fig. 4, rTS_A1, rTS_A2 and rTS_A3 correspond to passages 11,17 and 20, respectively). The early trophectoderm appeared distant from the rTSCs, as already observed for the early epiblast and derived pluripotent stem cells [51]. Interestingly, on the first PCA axis (41% of variance explained), the different trophoblast cells seem to form a differentiation trajectory from stem cells to the most differentiated ones grown on collagen (Fig. 4B). To get further insight into the nature of the different cells with regard to the trophectoderm, we compared the expression of a set of marker genes involved in lineage identity and trophoblast development in mouse and human, *i.e.*, the embryonic markers *POU5F1*, *NANOG* and *SOX2* [52,53]; the mouse trophoblast markers *CDX2* [54], *ESRRB* [55], and *TFAP2C* [56]; and the human early trophoblast markers *GATA2*, *GATA3*, *DAB2*, *TEAD3*, *KRT8* [57]. In addition, *RLN3* (relaxin), *PPARG* and *ORY1* (the rabbit syncytin) were added to the list for their role in trophoblast differentiation [45,58–61]. At last, *FURIN* was included as being involved in trophoblast stem cell (TSC) maintenance in mouse [62] and expressed in bovine trophoblast [63]. Clustering of the samples based on the expression of these selected genes grouped together rTSCs and the early trophoblast, confirming the trophoblastic

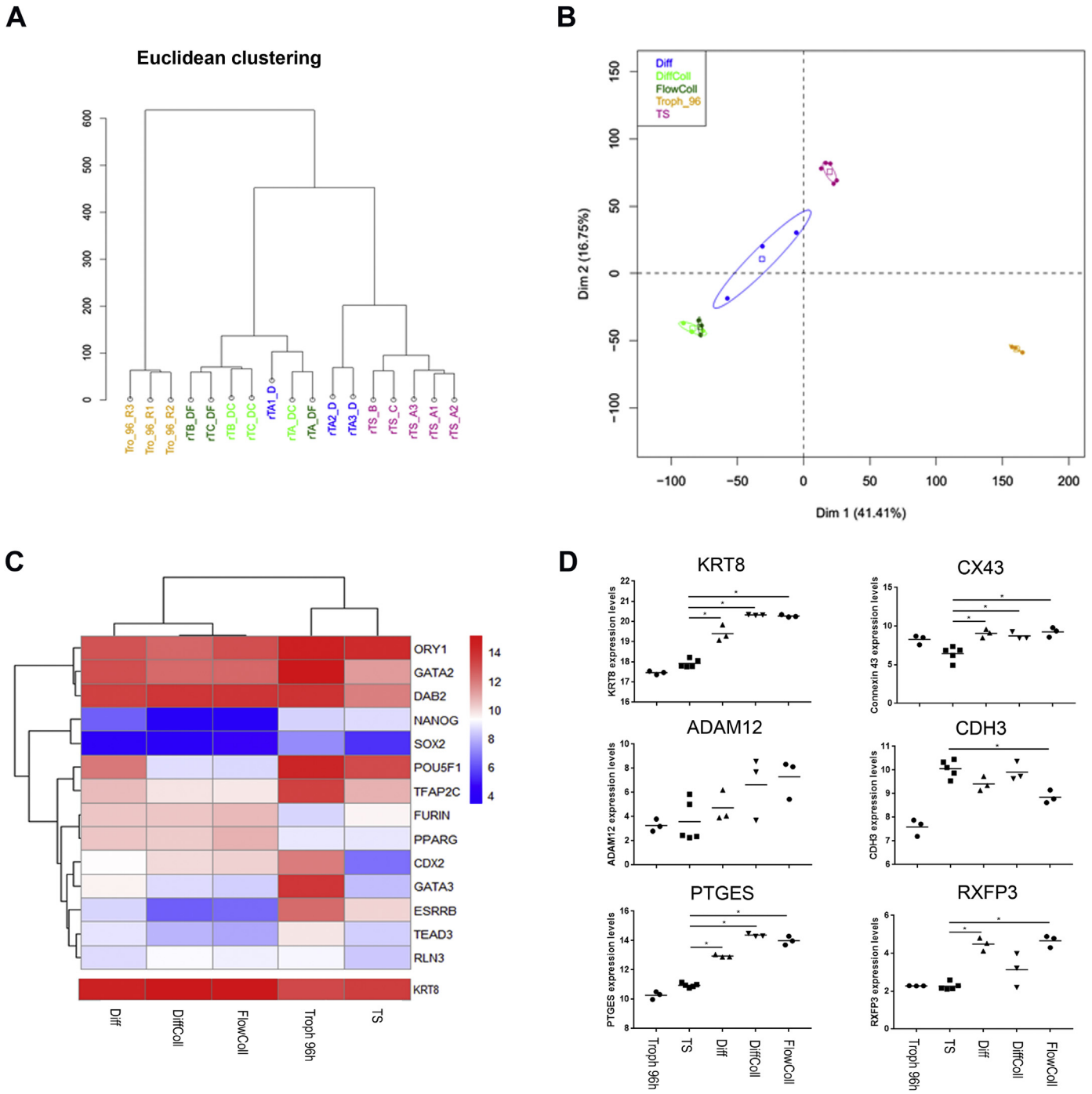

Fig. 4. Transcriptome analysis of trophoblast cells. A) Hierarchical clustering of the expression profiles of early trophectoderm of 96 h (Tro_96_R1, Tro_96_R2 and Tro_96_R3), rTSCs (rTS_A1, rTS_A2, rTS_A3, rTS_B and rTS_C) and the differentiated derivatives (rTA_DC, rTB_DC and rTC_DC for cells differentiated onto a collagen I gel; rTA_DF, rTB_DF and rTC_DF for cells differentiated onto a collagen I gel and with FSS; rTA1_D, rTA2_D and rTA3_D for cells differentiated without collagen nor FSS). B) Projection of samples according to their principal component analysis along the two first axes. C) Heatmap and hierarchical clustering based on the expression values (Rlog) of selected lineage and trophoblast differentiation markers. KRT8 was analyzed separately due to its very high expression level in all samples compared to other genes. Clustering was performed based on Pearson correlation and Ward linkage method. D) Dot plots showing the expression (Rlog) levels of some other selected genes. Relevant significant results (*P* values ≤ 0.05) were indicated. rTSCs (TS) were differentiated onto a collagen I gel with (FlowColl) or without (DiffColl) fluid shear stress (FSS), or without collagen gel nor FSS (Diff).

identity of the derived cells, and, as expected, the very low expression of the pluripotent markers *SOX2* and *NANOG* (Fig. 4C). The embryonic marker *POU5F1* was present in both rTSCs and early trophoblast, but was progressively lost during further differentiation, as previously observed *in vivo* [53,64]. Interestingly, the trophectoderm and the derived rTSCs displayed high expression of both mouse and human markers such as *TFAP2C*, *ESRRB*, *GATA2*, *KRT8* and *DAB2*. On the other hand, *GATA3*, *TEAD3* and *CDX2* were present *in vivo* but down-regulated during culture. Such a decline in the *in vitro* compared to *in vivo* expression was previously reported at least for *CDX2* in human TSCs [65,66]. *ESSRB* was the only marker to be strongly down-regulated in all differentiated cells. This is in line with its role in the mouse in the maintenance of a stem cell pool *in vivo* [67] and *in vitro* [55]. Conversely, the expression of two genes, *PPARG* and *FURIN*, was increased

in the differentiated cells. As mentioned before and in agreement, PPARG is known to play a role in trophoblast cell differentiation. Regarding *FURIN,* it is known to activate syncytin by cleaving the syncytin preprotein [59]. Hence, although syncytin (*ORY1*) expression did not change much during rTSCs differentiation, it may be more active in differentiated cells. Moreover, we noted that other proteins than syncytin involved in cell fusion tended to be more expressed in differentiated cells, such as *CX43* (*GJA1*) and *ADAM12* (Fig. 4D). Inversely and as expected when cell fusion occurs, cadherin *CDH3* expression tended to be reduced in differentiated cells grown with FSS (Fig. 4D). *RLN3* (relaxin) expression, known to be increased in rabbit syncytiotrophoblasts during gestation [68], was found modest at the transcriptional level in the various rabbit trophoblast cells, but slightly increased in cells differentiated on collagen (with and without FSS) compared to rTSCs. Moreover, the expression of the relaxin receptor 3, *RXFP3*, tended to be increased in all the differentiated cells compared to rTSCs (Fig. 4D).

Altogether, this focus on a set of marker genes demonstrated the trophoblastic origin of the derived cells and their ability to differentiate towards syncytiotrophoblasts.

4.4. Pathways involved in the differentiation of rTSCs

To further explore the changes in gene expression during *in vitro* differentiation of rTSCs, we determined the differentially expressed genes (DEG) between the different groups of cells. Overall, the differentiation process engaged a considerable number of genes (3106 up-regulated; 3073 down-regulated) between rTSCs and the various differentiated cells, with only partial overlap between conditions (Fig. 5A). In addition, the number of DEG specifically induced or down-regulated by collagen was about four times higher than simple differentiation on plastic (Fig. 5A). GO and KEGG term enrichment analysis was then performed for DEG during rTSC differentiation on collagen (DiffColl and FlowColl).

Downregulated DEG during differentiation of the rTSCs showed enriched terms related to cell division, DNA repair and protein synthesis, in agreement with the loss of stemness and the reduced proliferation of differentiated cells (Fig. 5B).

Terms upregulated in differentiated cells grown onto a collagen I gel compared to rTSCs were consistent with the differentiation process and trophoblast cell functions (Fig. 5B). Among these pathways, the PPAR signaling pathway was described to play a major role in trophoblast cell differentiation and functions and we suggest that it is involved in the observed FSS effects (Fig. 3A). In particular, the *PTGES* gene, that encodes PGE synthase, was upregulated in differentiated cells, and even more in cells grown onto a collagen matrix (Fig. 4D). This could lead to increased levels of PGE2 and thus of 15-keto-PGE2, which is a ligand of PPARγ. Also, the likely increase in the level of PGE2 could promote PPARγ activity through activation of adenylate cyclase. To further analyze this pathway, we compiled expression of its different components in rTSCs and their derivatives (Fig. 5D). *PPARG*, but also *PPARA* and *PPARD* were more expressed in the differentiated cells (Figs. 4C and 5D), as well as several genes of the PPAR signaling pathway involved in lipid transport, storage or metabolism (*CD36*, *PLIN2*, *FABP*, several *FATP* and *CYP* genes). Interestingly, several genes of the PPAR signaling pathway were more expressed with FSS, such as *PLIN2*, *CYP1B1*, *ASCL5* and *ANGPTL4* (Fig. 5D), involved in lipid metabolism, transport and storage, consistent with the increased lipid droplet accumulation induced by FSS. In particular, *CYP1B1* was reported to be regulated by the cAMP/PKA pathway [69,70] and its increased expression under FSS suggests that the cAMP/PKA signaling pathway is indeed induced by FSS in our culture model as proposed in Fig. 3A. In addition, the mechanosensitive TRPV6 channel was more expressed in the differentiated cells grown on collagen (with and without FSS) than in rTSCs (Fig. 5E). We thus assume that the mechanical forces exerted by the medium flow on differentiated cells activate this channel, leading to an increase in intracellular Ca^{2+} as shown in Fig. 3B, and to subsequent activation of the cAMP/PKA pathway, as well as to enhanced microvilli formation (as proposed in Fig. 3A). Moreover, while only a few genes were significantly upregulated upon FSS (Fig. 5A), gene ontology analysis revealed enrichment in steroid biosynthesis (Fig. 5C). This is an indication that the syncytiotrophoblasts formed under FSS are indeed functional, as it has been shown that these cells produce steroid hormones in Humans [36]. Likewise, we noticed that the ABC transporters were upregulated during differentiation (Fig. 5B), in agreement with the exchange function of the syncytiotrophoblasts. At last, we noted enrichment in pathways regulating actin cytoskeleton and sphingolipid metabolism, which may also account for the increased formation of microvilli during differentiation.

When gene ontology enrichment was performed on DEG between differentiated cells grown with or without collagen, the pathways that were mainly upregulated in the presence of a collagen gel concerned cell interactions with extracellular matrix (supplementary Fig. 3).

In conclusion, the functional analysis of DEG between rTSCs and their derivatives revealed signaling pathways involved in trophoblast cell differentiation and functions, especially on a collagen matrix, showing that collagen I promotes the differentiation of the rabbit trophoblast cells. In addition, at the transcriptional level, the FSS promotes the expression of some genes involved in the PPAR signaling pathway and in steroidogenesis.

5. Conclusion

In the present study, we derived rabbit TSCs from blastocysts and differentiated them into cells which express both phenotypic characteristics and marker genes of trophoblast cells. Especially, we succeeded in promoting cell differentiation by growing rTSCs on a collagen matrix and in the presence of a flow of culture medium that mimics the maternal blood flow. As already reported, we showed that the FSS exerted by the flow of culture medium promotes microvilli formation on the trophoblast cell surface, but, to our knowledge, we revealed for the first time that FSS also favors lipid droplet accumulation, and above all, trophoblast cell fusion to form the syncytiotrophoblast. Furthermore, at the transcriptional level, FSS promotes the expression of genes encoding steroidogenic enzymes, that may promote the steroid hormone production by the syncytiotrophoblast, as well as genes of the PPAR signaling pathway involved in trophoblast cell differentiation. Altogether, we believe that our cell culture model allows mimicking the *in vivo* conditions and could be used to study the differentiation of trophoblast stem cells into cytotrophoblasts and syncytiotrophoblasts, as well as the trophoblast function in physiological and pathological conditions.

Author contributions

GS supervised the study, designed and performed most of the experiments, analyzed the data and wrote the manuscript. ND participated in the derivation of rTSCs, in cell culture and in the writing. CA performed some RNA isolations, the RNA quality control and participated in the transcriptomic data analysis. MCA participated in cell culture. YJ performed the RNA sequencing. VD participated in the transcriptomic data acquisition and analysis and in the writing. PCP facilitated the contacts and participated in the writing. AJ participated in the derivation of rTSCs, performed the major part of the transcriptomic data analysis with the help of LJ and participated in the writing. All authors reviewed and approved the manuscript.

Funding

This work was supported by the Institut National de la Recherche Agronomique (INRA), a funding provided by the INRA PHASE department, and by ANR Programme Investissements d'Avenir REVIVE ANR-10-LABX73.

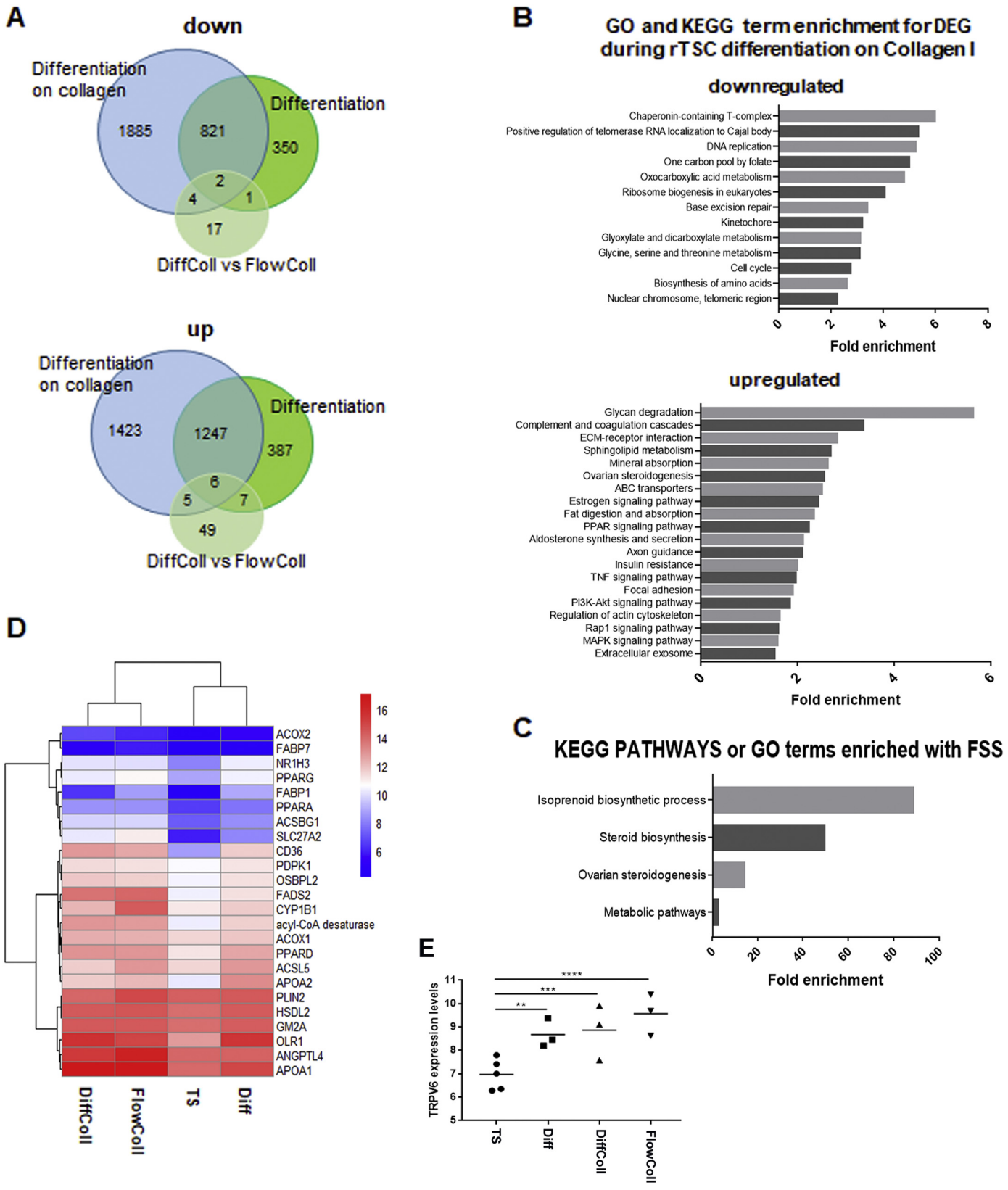

Fig. 5. Differentially expressed genes in trophoblast cells. rTSCs (TS) were differentiated onto a collagen I gel with (FlowColl) or without (DiffColl) fluid shear stress (FSS), or without collagen gel nor FSS (Diff). A) Venn diagrams showing the overlap between DEG of the different comparisons: during differentiation of rTSCs on collagen (Differentiation on Collagen) or on non-coated plate (Differentiation), and under FSS (DiffColl *vs* FlowColl). B) Enriched terms in rTSCs (downregulated) or in cells on collagen (upregulated). C) Enriched terms in DEG upregulated under FSS. In B and C, only terms with a Benjamini adjusted P value ≤ 0.05 are depicted. D) Heatmap of selected genes belonging to the PPAR pathway. Clustering was performed based on Pearson correlation and Ward linkage method. E) Dot plots showing the expression (Rlog) levels of the TRPV6 gene in the various cells. Relevant significant results (adjusted P values from differential analysis ≤ 0.05) were indicated.

Acknowledgments

We thank Vincent Brochard for the preparation of mouse embryonic fibroblasts and Christophe Sanz for FSS value estimations. We also thank the MIMA2 platform for access to confocal microscopy and Pierre Adenot and Martine Letheule for their help on confocal microscopy observations. We acknowledge the high-throughput sequencing facility of I2BC for its sequencing and bioinformatics expertise and for its contribution to this study.

Disclosure of Potential Conflicts of Interest

the authors have nothing to disclose.

Appendix A. Supplementary data

Supplementary data to this article can be found online at https://doi.org/10.1016/j.bbagen.2019.07.003.

References

[1] G.J. Burton, A.L. Fowden, K.L. Thornburg, Placental origins of chronic disease, Physiol. Rev. 96 (2016) 1509–1565.
[2] K.L. Thornburg, K. Kolahi, M. Pierce, A. Valent, R. Drake, S. Louey, Biological features of placental programming, Placenta 48 (Suppl. 1) (2016) S47–S53.
[3] J.L. James, A.M. Carter, L.W. Chamley, Human placentation from nidation to 5 weeks of gestation. Part I: what do we know about formative placental development following implantation? Placenta 33 (2012) 327–334.
[4] M.Y. Turco, L. Gardner, R.G. Kay, R.S. Hamilton, M. Prater, M.S. Hollinshead, A. McWhinnie, L. Esposito, R. Fernando, H. Skelton, F. Reimann, F.M. Gribble, A. Sharkey, S.G.E. Marsh, S. O'Rahilly, M. Hemberger, G.J. Burton, A. Moffett, Trophoblast organoids as a model for maternal-fetal interactions during human placentation, Nature 564 (2018) 263–267.
[5] L. Aengenheister, K. Keevend, C. Muoth, R. Schonenberger, L. Diener, P. Wick, T. Buerki-Thurnherr, An advanced human in vitro co-culture model for translocation studies across the placental barrier, Sci. Rep. 8 (2018) 5388.
[6] C. Blundell, E.R. Tess, A.S. Schanzer, C. Coutifaris, E.J. Su, S. Parry, D. Huh, A microphysiological model of the human placental barrier, Lab Chip 16 (2016) 3065–3073.
[7] J.S. Lee, R. Romero, Y.M. Han, H.C. Kim, C.J. Kim, J.S. Hong, D. Huh, Placenta-on-a-chip: a novel platform to study the biology of the human placenta, J. Matern. Fetal Neonatal Med. 29 (2016) 1046–1054.
[8] L. Li, D.J. Schust, Isolation, purification and in vitro differentiation of cytotrophoblast cells from human term placenta, Reprod. Biol. Endocrinol. 13 (2015) 71.
[9] F. Liu, M.J. Soares, K.L. Audus, Permeability properties of monolayers of the human trophoblast cell line BeWo, Am. J. Phys. 273 (1997) C1596–C1604.
[10] C.A. McConkey, E. Delorme-Axford, C.A. Nickerson, K.S. Kim, Y. Sadovsky, J.P. Boyle, C.B. Coyne, A three-dimensional culture system recapitulates placental syncytiotrophoblast development and microbial resistance, Sci. Adv. 2 (2016) e1501462.
[11] S. Miura, K. Sato, M. Kato-Negishi, T. Teshima, S. Takeuchi, Fluid shear triggers microvilli formation via mechanosensitive activation of TRPV6, Nat. Commun. 6 (2015) 8871.
[12] C. Muoth, A. Wichser, M. Monopoli, M. Correia, N. Ehrlich, K. Loeschner, A. Gallud, M. Kucki, L. Diener, P. Manser, W. Jochum, P. Wick, T. Buerki-Thurnherr, A 3D co-culture microtissue model of the human placenta for nanotoxicity assessment, Nanoscale 8 (2016) 17322–17332.
[13] F. Yin, Y. Zhu, M. Zhang, H. Yu, W. Chen, J. Qin, A 3D human placenta-on-a-chip model to probe nanoparticle exposure at the placental barrier, Toxicol. in Vitro 54 (2018) 105–113.
[14] S. Furukawa, Y. Kuroda, A. Sugiyama, A comparison of the histological structure of the placenta in experimental animals, J. Toxicol. Pathol. 27 (2014) 11–18.
[15] J.D. Boyd, W.J. Hamilton, Development and structure of the human placenta from the end of the 3rd month of gestation, J Obstet Gynaecol Br Commonw 74 (1967) 161–226.
[16] A. Tarrade, P. Chavatte-Palmer, M. Guillomot, S. Camous, D. Evain-Brion, La reproduction animale et humaine, Chapter 20 Le placenta, Editions Quae, (2014), pp. 367–392.
[17] A. Malassine, J.L. Frendo, D. Evain-Brion, A comparison of placental development and endocrine functions between the human and mouse model, Hum. Reprod. Update 9 (2003) 531–539.
[18] P. Chavatte-Palmer, A. Tarrade, Placentation in different mammalian species, Ann Endocrinol (Paris) 77 (2016) 67–74.
[19] E. Lecarpentier, A. Atallah, J. Guibourdenche, M. Hebert-Schuster, S. Vieillefosse, A. Chissey, B. Haddad, G. Pidoux, D. Evain-Brion, A. Barakat, T. Fournier, V. Tsatsaris, Fluid shear stress promotes placental growth factor upregulation in human Syncytiotrophoblast through the cAMP-PKA signaling pathway, Hypertension 68 (2016) 1438–1446.
[20] F.C. Morales, Y. Takahashi, E.L. Kreimann, M.M. Georgescu, Ezrin-radixin-moesin (ERM)-binding phosphoprotein 50 organizes ERM proteins at the apical membrane of polarized epithelia, Proc. Natl. Acad. Sci. U. S. A. 101 (2004) 17705–17710.
[21] I. Saotome, M. Curto, A.I. McClatchey, Ezrin is essential for epithelial organization and villus morphogenesis in the developing intestine, Dev. Cell 6 (2004) 855–864.
[22] O. De Wever, A. Hendrix, A. De Boeck, W. Westbroek, G. Braems, S. Emami, M. Sabbah, C. Gespach, M. Bracke, Modeling and quantification of cancer cell invasion through collagen type I matrices, Int J Dev Biol 54 (2010) 887–896.
[23] E. Lecarpentier, M. Bhatt, G.I. Bertin, B. Deloison, L.J. Salomon, P. Deloron, T. Fournier, A.I. Barakat, V. Tsatsaris, Computational fluid dynamic simulations of maternal circulation: wall shear stress in the human placenta and its biological implications, PLoS One 11 (2016) e0147262.
[24] G.J. Burton, A.W. Woods, E. Jauniaux, J.C. Kingdom, Rheological and physiological consequences of conversion of the maternal spiral arteries for uteroplacental blood flow during human pregnancy, Placenta 30 (2009) 473–482.
[25] G. Sanz, C. Schlegel, J.C. Pernollet, L. Briand, Comparison of odorant specificity of two human olfactory receptors from different phylogenetic classes and evidence for antagonism, Chem. Senses 30 (2005) 69–80.
[26] G. Launay, S. Teletchea, F. Wade, E. Pajot-Augy, J.F. Gibrat, G. Sanz, Automatic modeling of mammalian olfactory receptors and docking of odorants, Protein Eng Des Sel 25 (2012) 377–386.
[27] F. Heidebrecht, I. Schulz, M. Keller, S.E. Behrens, A. Bader, Improved protocols for protein and RNA isolation from three-dimensional collagen sandwich cultures of primary hepatocytes, Anal. Biochem. 393 (2009) 141–144.
[28] S. Lê, J. Josse, F. Husson, FactoMineR: an R package for multivariate analysis, J. Stat. Softw. 25 (2008) 1–18.
[29] S. Anders, W. Huber, Differential expression analysis for sequence count data, Genome Biol. 11 (2010) R106.
[30] W. Huang da, B.T. Sherman, R.A. Lempicki, Systematic and integrative analysis of large gene lists using DAVID bioinformatics resources, Nat. Protoc. 4 (2009) 44–57.
[31] S. Tanaka, T. Kunath, A.K. Hadjantonakis, A. Nagy, J. Rossant, Promotion of trophoblast stem cell proliferation by FGF4, Science 282 (1998) 2072–2075.
[32] A. Erlebacher, K.A. Price, L.H. Glimcher, Maintenance of mouse trophoblast stem cell proliferation by TGF-beta/activin, Dev. Biol. 275 (2004) 158–169.
[33] T. Tan, X. Tang, J. Zhang, Y. Niu, H. Chen, B. Li, Q. Wei, W. Ji, Generation of trophoblast stem cells from rabbit embryonic stem cells with BMP4, PLoS One 6 (2011) e17124.
[34] J.L. Jameson, A.N. Hollenberg, Regulation of chorionic gonadotropin gene expression, Endocr. Rev. 14 (1993) 203–221.
[35] W.T. Schaiff, M.G. Carlson, S.D. Smith, R. Levy, D.M. Nelson, Y. Sadovsky, Peroxisome proliferator-activated receptor-gamma modulates differentiation of human trophoblast in a ligand-specific manner, J. Clin. Endocrinol. Metab. 85 (2000) 3874–3881.
[36] A. Tarrade, K. Schoonjans, J. Guibourdenche, J.M. Bidart, M. Vidaud, J. Auwerx, C. Rochette-Egly, D. Evain-Brion, PPAR gamma/RXR alpha heterodimers are involved in human CG beta synthesis and human trophoblast differentiation, Endocrinology 142 (2001) 4504–4514.
[37] Y. Barak, M.C. Nelson, E.S. Ong, Y.Z. Jones, P. Ruiz-Lozano, K.R. Chien, A. Koder, R.M. Evans, PPAR gamma is required for placental, cardiac, and adipose tissue development, Mol. Cell 4 (1999) 585–595.
[38] B. Wice, D. Menton, H. Geuze, A.L. Schwartz, Modulators of cyclic AMP metabolism induce syncytiotrophoblast formation in vitro, Exp. Cell Res. 186 (1990) 306–316.
[39] M.F. Diaz, N. Li, H.J. Lee, L. Adamo, S.M. Evans, H.E. Willey, N. Arora, Y.S. Torisawa, D.A. Vickers, S.A. Morris, O. Naveiras, S.K. Murthy, D.E. Ingber, G.Q. Daley, G. Garcia-Cardena, P.L. Wenzel, Biomechanical forces promote blood development through prostaglandin E2 and the cAMP-PKA signaling axis, J. Exp. Med. 212 (2015) 665–680.
[40] M.J. Duchesne, H. Thaler-Dao, A.C. de Paulet, Prostaglandin synthesis in human placenta and fetal membranes, Prostaglandins 15 (1978) 19–42.
[41] W.L. Chou, L.M. Chuang, C.C. Chou, A.H. Wang, J.A. Lawson, G.A. FitzGerald, Z.F. Chang, Identification of a novel prostaglandin reductase reveals the involvement of prostaglandin E2 catabolism in regulation of peroxisome proliferator-activated receptor gamma activation, J. Biol. Chem. 282 (2007) 18162–18172.
[42] Y. Barak, Y. Sadovsky, T. Shalom-Barak, PPAR signaling in placental development and function, PPAR Res. 2008 (2008) 142082.
[43] I. Knerr, S.W. Schubert, C. Wich, K. Amann, T. Aigner, T. Vogler, R. Jung, J. Dotsch, W. Rascher, S. Hashemolhosseini, Stimulation of GCMa and syncytin via cAMP mediated PKA signaling in human trophoblastic cells under normoxic and hypoxic conditions, FEBS Lett. 579 (2005) 3991–3998.
[44] K. Levytska, S. Drewlo, D. Baczyk, J. Kingdom, PPAR- gamma regulates trophoblast differentiation in the BeWo cell model, PPAR Res., 2014 (2014) 637251.
[45] M. Ruebner, M. Langbein, P.L. Strissel, C. Henke, D. Schmidt, T.W. Goecke, F. Faschingbauer, R.L. Schild, M.W. Beckmann, R. Strick, Regulation of the human endogenous retroviral Syncytin-1 and cell-cell fusion by the nuclear hormone receptors PPARgamma/RXRalpha in placentogenesis, J. Cell. Biochem. 113 (2012) 2383–2396.
[46] C. Yu, K. Shen, M. Lin, P. Chen, C. Lin, G.D. Chang, H. Chen, GCMa regulates the syncytin-mediated trophoblastic fusion, J. Biol. Chem. 277 (2002) 50062–50068.
[47] L. Woods, V. Perez-Garcia, M. Hemberger, Regulation of placental development and its impact on fetal growth-new insights from mouse models, Front Endocrinol (Lausanne) 9 (2018) 570.
[48] A. Gil-Sanchez, H. Demmelmair, J.J. Parrilla, B. Koletzko, E. Larque, Mechanisms involved in the selective transfer of long chain polyunsaturated fatty acids to the fetus, Front. Genet. 2 (2011) 57.
[49] E. Herrera, H. Ortega-Senovilla, Lipid metabolism during pregnancy and its implications for fetal growth, Curr. Pharm. Biotechnol. 15 (2014) 24–31.
[50] C.S. Roland, J. Hu, C.E. Ren, H. Chen, J. Li, M.S. Varvoutis, L.W. Leaphart,

D.B. Byck, X. Zhu, S.W. Jiang, Morphological changes of placental syncytium and their implications for the pathogenesis of preeclampsia, Cell. Mol. Life Sci. 73 (2016) 365–376.
[51] B. Schmaltz-Panneau, L. Jouneau, P. Osteil, Y. Tapponnier, M. Afanassieff, M. Moroldo, A. Jouneau, N. Daniel, C. Archilla, P. Savatier, V. Duranthon, Contrasting transcriptome landscapes of rabbit pluripotent stem cells in vitro and in vivo, Anim. Reprod. Sci. 149 (2014) 67–79.
[52] A. Piliszek, Z.E. Madeja, B. Plusa, Suppression of ERK signalling abolishes primitive endoderm formation but does not promote pluripotency in rabbit embryo, Development 144 (2017) 3719–3730.
[53] C.H. Chen, J. Xu, W.F. Chang, C.C. Liu, H.Y. Su, Y.E. Chen, F. Du, L.Y. Sung, Dynamic profiles of Oct-4, Cdx-2 and acetylated H4K5 in in-vivo-derived rabbit embryos, Reprod. BioMed. Online 25 (2012) 358–370.
[54] D. Strumpf, C.A. Mao, Y. Yamanaka, A. Ralston, K. Chawengsaksophak, F. Beck, J. Rossant, Cdx2 is required for correct cell fate specification and differentiation of trophectoderm in the mouse blastocyst, Development 132 (2005) 2093–2102.
[55] P.A. Latos, A. Goncalves, D. Oxley, H. Mohammed, E. Turro, M. Hemberger, Fgf and Esrrb integrate epigenetic and transcriptional networks that regulate self-renewal of trophoblast stem cells, Nat. Commun. 6 (2015) 7776.
[56] P. Kuckenberg, S. Buhl, T. Woynecki, B. van Furden, E. Tolkunova, F. Seiffe, M. Moser, A. Tomilin, E. Winterhager, H. Schorle, The transcription factor TCFAP2C/AP-2gamma cooperates with CDX2 to maintain trophectoderm formation, Mol. Cell. Biol. 30 (2010) 3310–3320.
[57] G.G. Stirparo, T. Boroviak, G. Guo, J. Nichols, A. Smith, P. Bertone, Correction: integrated analysis of single-cell embryo data yields a unified transcriptome signature for the human pre-implantation epiblast (doi: 10.1242/dev.158501), Development 145 (2018).
[58] V.H. Lee, S.J. Zhang, S.M. Chang, M.J. Fields, P.A. Fields, In vitro transformation of rabbit cytotrophoblast cells into syncytiotrophoblast: stimulation of hormone secretion by progesterone and dibutyryl cyclic 3′,5′-adenosine monophosphate, Biol. Reprod. 52 (1995) 868–877.
[59] A.J. Potgens, S. Drewlo, M. Kokozidou, P. Kaufmann, Syncytin: the major regulator of trophoblast fusion? Recent developments and hypotheses on its action, Hum. Reprod. Update 10 (2004) 487–496.
[60] A. Dupressoir, C. Lavialle, T. Heidmann, From ancestral infectious retroviruses to bona fide cellular genes: role of the captured syncytins in placentation, Placenta 33 (2012) 663–671.
[61] O. Heidmann, C. Vernochet, A. Dupressoir, T. Heidmann, Identification of an endogenous retroviral envelope gene with fusogenic activity and placenta-specific expression in the rabbit: a new "syncytin" in a third order of mammals, Retrovirology 6 (2009) 107.
[62] M. Guzman-Ayala, N. Ben-Haim, S. Beck, D.B. Constam, Nodal protein processing and fibroblast growth factor 4 synergize to maintain a trophoblast stem cell microenvironment, Proc. Natl. Acad. Sci. U. S. A. 101 (2004) 15656–15660.
[63] S.A. Degrelle, E. Campion, C. Cabau, F. Piumi, P. Reinaud, C. Richard, J.P. Renard, I. Hue, Molecular evidence for a critical period in mural trophoblast development in bovine blastocysts, Dev. Biol. 288 (2005) 448–460.
[64] E. Canon, L. Jouneau, T. Blachere, N. Peynot, N. Daniel, L. Boulanger, L. Maulny, C. Archilla, S. Voisin, A. Jouneau, M. Godet, V. Duranthon, Progressive methylation of POU5F1 regulatory regions during blastocyst development, Reproduction 156 (2018) 145–161.
[65] S. Haider, G. Meinhardt, L. Saleh, V. Kunihs, M. Gamperl, U. Kaindl, A. Ellinger, T.R. Burkard, C. Fiala, J. Pollheimer, S. Mendjan, P.A. Latos, M. Knofler, Self-renewing trophoblast organoids recapitulate the developmental program of the early human placenta, Stem Cell Reports 11 (2018) 537–551.
[66] H. Okae, H. Toh, T. Sato, H. Hiura, S. Takahashi, K. Shirane, Y. Kabayama, M. Suyama, H. Sasaki, T. Arima, Derivation of human trophoblast stem cells, Cell Stem Cell 22 (2018) 50–63 (e56).
[67] J. Luo, R. Sladek, J.A. Bader, A. Matthyssen, J. Rossant, V. Giguere, Placental abnormalities in mouse embryos lacking the orphan nuclear receptor ERR-beta, Nature 388 (1997) 778–782.
[68] R.K. Eldridge, P.A. Fields, Rabbit placental relaxin: purification and immunohistochemical localization, Endocrinology 117 (1985) 2512–2519.
[69] S. Deb, S.M. Bandiera, Regulation of cytochrome P450 1B1 expression by luteinizing hormone in mouse MA-10 and rat R2C Leydig cells: role of protein kinase a, Biol. Reprod. 85 (2011) 89–96.
[70] W. Zheng, T. Tong, J. Lee, X. Liu, C. Marcus, C.R. Jefcoate, Stimulation of mouse Cyp1b1 during adipogenesis: characterization of promoter activation by the transcription factor Pax6, Arch. Biochem. Biophys. 532 (2013) 1–14.